X-615-68-262
PREPRINT

NASA TM X- 63286

NITRIC OXIDE IN THE MESOSPHERE AND ITS VARIATIONS

A. P. MITRA

JULY 1968

GODDARD SPACE FLIGHT CENTER
GREENBELT, MARYLAND

Invited Paper for COSPAR-IAMAP Joint Session on "Problems of the Winter Atmosphere from the Stratosphere to the Turbopause" COSPAR Assembly, Tokyo, May 1968

NITRIC OXIDE IN THE MESOSPHERE AND ITS VARIATIONS

A. P. Mitra*
Laboratory for Space Sciences
NASA Goddard Space Flight Center
Greenbelt, Maryland

The distributions, seasonal variations and the resulting ionospheric implications of mesospheric nitric oxide are discussed. We first consider the principal features of an average distribution for this constituent that would be consistent with photochemical considerations and with the diurnal and solar cycle variations in D region ionization and the relative abundances of the molecular ions NO^+ and O_2^+.

We then consider the extent to which the average profile may vary seasonally in middle latitudes. Large winter enhancements occur in NO concentrations at all D region heights above about 70 km due to the winter warming at these heights. The enhanced region is limited roughly between 70-90 km, the lower limit being controlled by the rapid loss of nitric oxide through ozone. NO production through the ionic reaction $O_2^+ + N_2 \rightarrow NO^+ + NO$ does not appear to be significant at any height.

Ionospheric implications of these NO distributions are also discussed.

---

*NRC-NASA Resident Research Associate, on leave from the National Physical Laboratory, New Delhi 12, India.

INTRODUCTION

An important question concerning mesospheric ionization and meteorology is the role played by such minor constituents as nitric oxide, ozone and atomic oxygen, the metallic species, water vapour and ion clusters, and certain excited states of the principal constituents. The importance of these in the ionization of the mesosphere is now, in most cases, clearly established.

In this work we deal with the distributions, variations and the resulting ionospheric implications of only one of these minor constituents, eg. nitric oxide.

Information on the distribution of nitric oxide in the mesosphere and the lower thermosphere has been obtained in three ways: from rocket measurements of nitric oxide airglow in a series of flights by Barth (1966), from photochemical considerations (Nicolet, 1965; Barth, 1961; Wagner, 1966), from changes in the D region electron density profiles with solar activity (Mitra, 1966) and with the time of the day (Mitra, 1968) and from pre-sunrise measurements of E region electron density (Smith, 1966). In an earlier work (Mitra, 1968) in which estimates from these different sources have been reviewed, the following empirical distribution was suggested:

$$n(NO) = 4\times10^{-1} n(O_2) e^{-3700/T} + 5\times10^{-7} n(O) \qquad (1)$$

In this work we will obtain some additional ionospheric estimates for mesospheric nitric oxide. We find that these new values are generally consistent with our previous empirical model, escept in the region of minimum around80-100 km, where the new values are larger. We then examine the changes that are likely to occur in this distribution in winter from known changes in the distribution of atmospheric temperature and in the concentrations of atomic oxygen and ozone. The resulting concentrations in winter are found to be considerably larger than in summer, at heights between 70-90 km, the exact degree of enhancement being dependent on latitude. The consequences of such changes in the ionization of the winter mesosphere are found to be quite severe.

2. AN AVERAGE DISTRIBUTION FOR NITRIC OXIDE IN THE MESOSPHERE AND THE LOWER THERMOSPHERE

Currently available estimates of the nitric oxide concentration in the mesosphere and the lower thermosphere, and the sources from which these are derived, are given in Appendix 1.

The unusually large value obtained in Barth's measurement has been frequently discussed. In contrast, the different ionospheric estimates listed in Appendix 1 are found to be generally consistent and in agreement with photochemically deduced values.

The ionospheric estimates are, however, still far from definitive, although these are probably reliable as order-of-magnitude values. If the major source in a non-polar latitude changes from cosmic rays to Lα to X rays as one moves from the lower to higher mesosphere, then the problem of obtaining a reliable value for NO reduces to one of identifying the height at which ionization by Lα predominates. This, it appears, can at present be best done from an examination of the diurnal variation of electron density profiles. In our previous study we used the diurnal profiles obtained by Barrington et al (1963) for the high latitude station Kjeller for the period March 17 to April 7, 1960. This identified the Lα-dominated levels to be around 72 km. A more recent series of results, which we examine here in detail, comes from Thrane et al (1968) who obtained detailed profiles of mesospheric ionization for a large range of χ values, for both afternoon and morning conditions, from partial reflection and cross-modulation experiments conducted in the middle latitudes during the IQSY. The afternoon values were nearly the same as the morning values (for the same value of χ), thus making it possible to use N^2 directly as a measure of q, the electron production rate. Plots of N^2 against sec χ for the heights 65, 70 and 75 km are shown in Fig. 1, along with the theoretical variation expected from ionization controlled only by Lα radiation (assuming no diurnal variation for nitric

oxide). We again observe a variation essentially identical with that of Lα at 70 km, a slower variation at 65 km (as would be expected if cosmic ray contribution is also important) and a faster variation at 75 km, identical with that expected from ionization by X rays at $4A^{o}$.

From the results of Fig. 1, we obtain:

$$n(NO) \geq 5 \times 10^{6} \text{ cm}^{-3} \text{ at 70 km}$$

$$n(NO) = 4 \times 10^{8} \text{ cm}^{-3} \text{ at 65 km (probable value -not reliable)}$$

In all these estimates, as well as in our previous ones (Mitra, 1966; Mitra, 1968), the principal concern was to avoid any assumption of the loss rate Ψ, given by $\Psi = (1+\lambda)(\alpha_D + \lambda\alpha_i)$ where λ is the ratio of negative ions to electrons, α_i is the ion-ion recombination coefficient and α_D is the coefficient for dissociative recombination. This was done because of the current uncertainty in our knowledge of Ψ. Nevertheless, a lower limit for the electron production rate can be obtained by writing $\lambda=0$ in the equation:

$$q_c + q_L + q_x = (1+\lambda)(\alpha_D + \lambda\alpha_i)N^2 \qquad (4)$$

If we now limit ourselves to 70 km, for which q_x is negligible, then the <u>minimum</u> value for nitric oxide is set by the equation:

$$n(NO) = \frac{\alpha_D(NO^+)N^2}{Y(\chi)} - \frac{q_c}{Y(\chi)} \qquad (5)$$

where $Y(\chi) = A(NO)\, Q_\alpha(L\alpha)e^{-\tau(O_2,\chi)}$ defines the ionization yield due to Lα for one NO molecule.

Estimates of the quantity $N^2/Y(\chi)$ from observed electron densities at 70 km, over a wide range of solar zenith angles, give values in the range $(1\text{-}3)\times10^{12}cm^{-6}sec$, although abnormally large values around $50\times10^{12}cm^{-6}sec^{-1}$ are also occasionally encountered. If $q_c<\alpha_D(NO^+)N^2$, and one takes $\alpha_D(NO^+) = 5\times10^{-7}(T/300)^{-1.2}cm^3/s$ (see also sec. 3), then $\alpha_D(NO^+)$ at 70 km is around $7\times10^{-7}cm^3/s$, and

$$n(NO) \geq (0.7\text{-}2)\times10^6cm^{-3}$$

With Mitra's values (1968) of $\Psi(= 2\times10^{-6}cm^3/s)$ at 70 km,

$$n(NO) \approx (1.4\text{-}4)\times10^6cm^{-3}$$

A method of considerable value is the use of observations of NO^+ concentrations, which are now being available with increasing reliability, along with the laboratory measurements of rate coefficients relevant in NO^+ chemistry (Mitra, 1968; see also Appendix 1). The reactions relevant in the mesosphere are given in Table 1, along with the laboratory values of the rate coefficients, where available. It can be shown that NO concentration is related to the NO^+ concentration in the

TABLE 1

PRINCIPAL REACTIONS FOR NO^+ CHEMISTRY IN THE MESOSPHERE AND THE LOWER THERMOSPHERE

$NO + h\nu \longrightarrow NO^+ + e$	$q(NO)$
$O_2^+ + N_2 \xrightarrow{\gamma_7} NO^+ + NO$	$<10^{-15}(\sim 10^{-17\pm 2})\ cm^3/s$
$O_2^+ + NO \xrightarrow{\gamma_5} NO^+ + O_2$	$(8\pm 2)\times 10^{-10}\ cm^3/s$
$N_2^+ + O \xrightarrow{\gamma_{11}} NO^+ + N$	$(2.5\pm 0.8)\times 10^{-10}\ cm^3/s$
$N_2^+ + O_2 \xrightarrow{\gamma_9} O_2^+ + N_2$	$(2\pm 1)\times 10^{-10}\ cm^3/s$
$O^+ + N_2 \xrightarrow{\gamma_1} NO^+ + N$	$1\times 10^{-12\pm 0.5}\ cm^3/s$

mesosphere through the relation:

$$n(NO)[Y(\chi)+\gamma_5 n(O_2^+)]+\gamma_7 n(O_2^+)n(N_2)+q(N_2)\left[\frac{\gamma_{11}n(O)}{\gamma_{11}n(O)+\gamma_9 n(O_2)}\right. = \alpha_D(NO^+)n(NO^+)N_e \qquad (6)$$

where the quantity on the right hand side is directly obtained from observations.

With the rate coefficients given in Table 3, Eq. (6) takes the form:

$$A(\chi,O_2^+)n(NO)=\alpha_D(NO^+)n(NO^+)N_e-10^{-18}n(N_2)n(O_2^+)-B(O_2/O)q(N_2) \qquad (7)$$

with

$$A(\chi,O_2^+) = Y(\chi)+8\times 10^{-10}n(O_2^+)$$

$$B(O_2/O) = [1+n(O_2)/n(O)]^{-1}$$

Since O_2^+ is not observed below 80 km, and only exists in negligible quantity in the upper mesosphere, the second term on the right has no controlling effect in the expression and the uncertainty in the value of γ_7 has little effect on the determination NO concentration. Direct photoionization of NO ceases to be important in NO^+ chemistry above 80 km, but the neutral nitric oxide can still control NO^+ through process (O_2^++NO). Excepting for conditions of enhanced nitric oxide, the left hand side is negligible above about 100-120 km, and consequently the method ceases to be valid above this height.

Nitric oxide distribution has been computed on the basis of Eq. (6), using NO^+ distribution obtained by Narcisi and Bailey (1965) and with two sets of values for $\alpha_D(NO^+)$: (a) $\alpha_D(NO^+)=5\times10^{-7}(T/300)^{-1.2}cm^3/s$ and (b) a constant value of $2\times10^{-7}cm^3/s$. The distributions so derived are shown in Fig. 2 along with other estimates made in this and in previous works. For λ, a value of 6 (following Hale, 1968) is used for 70 km and 1 for 75 km. The distributions are nearly constant with concentrations around $6\times10^6cm^{-3}$ for (a) and $1.5\times10^6cm^{-3}$ for (b) between 70-80 km; the concentrations increase to about $3\times10^7cm^{-3}$ at 90 km for (a) and to $7\times10^6cm^{-3}$ for (b).

There is considerable agreement between these values and the simplest photochemical calculations. The major reactions

TABLE 2

PRINCIPAL REACTIONS FOR NITRIC OXIDE IN THE MESOSPHERE AND LOWER THERMOSPHERE

MAJOR REACTIONS

1.	$N+O_2 \xrightarrow{b_7} NO+O$	$b_7=(1.4\pm0.2)\times10^{-11}e^{-\frac{3600\pm200}{T}}$ cm^3/s
2.	$N+O+M \xrightarrow{b_{1a}} NO+M$	$b_{1a}=1.1\times10^{-32}(\frac{T}{300})$ cm^6/s
3.	$N+O \xrightarrow{b_{1b}} NO+h\nu$	$b_{1b}=2.10^{-17}$cm^3/s
4.	$N+NO \xrightarrow{b_6} N_2+O$	$b_6=2.2\times10^{-11}$cm^3/s
5.	$N+O_2(^1\Delta) \xrightarrow{k} NO+O$	k unknown (10^{-13}-10^{-15}cm^3/s used here)

ADDITIONAL PROCESSES LIKELY TO BE IMPORTANT

6.	$O_2^+ + N_2 \xrightarrow{\gamma_7} NO^+ + NO$	$\gamma_7=1\times10^{-17\pm2}$cm^3/s
7.	$NO+O_3 \xrightarrow{b_4} NO_2+O_2$	$b_4=9.5\times10^{-13}e^{-\frac{1300\pm100}{T}}$ cm^3/s
8.	$O_2^+ + NO \xrightarrow{\gamma_5} NO^+ + O_2$	$\gamma_5=(8\pm2)\times10^{-10}$cm^3/s

NO - DISTRIBUTIONS

1. Mitra's Empirical Distribution:

$$n(NO)=4\times10^{-1}\exp(-\frac{3700}{T})n(O_2)+5\times10^{-7}n(O)$$

2. Photochemical Equilibrium with 1-4:

$$n^*(NO)=(0.6\pm2)\times10^{-1}\exp(-\frac{3600\pm200}{T})n(O_2)$$

$$+[(1\pm0.5)\times10^{-6}+5\times10^{-21}n(M)\frac{T}{300}]n(O)$$

3. Photochemical Equilibrium - all processes 1-8:

$$n(NO)=n^*(NO)\left[\frac{1+\frac{kn[O_2(^1\Delta)]}{b_7n(O_2)+b_1n(O)}+\frac{\gamma_7}{b_1}\frac{n(O_2^+)n(N_2)}{n(O)n(N)}}{1+\frac{b_4}{b_6}\frac{n(O_3)}{n(N)}}\right]$$

involved in NO photochemistry are given in Table 2 along with distributions expected under photochemical equilibrium when the major processes are limited to 1-4 and in the more complex case including the effect of ionic reactions, possible production of NO from the metastable $O_2(^1\Delta)$ (Hunten and McElroy, 1968), and the very rapid loss of NO through ozone in the lower mesosphere.

In Figs. 3 and 4 the rates of production of NO (per nitrogen atom) and of loss (per NO molecule) are plotted as a function of height for heights between 50-120 km. For process $(O_2^+ + N_2)$ the rate has been normalized by dividing the total rate by n(N). For O_2, N_2 and O the distributions used are those given by CIRA 1965; for O_3, that given by Maeda and Aikin (1967) and for $O_2(^1\Delta)$, that obtained from the dayglow measurements of Evans et al (1968). For atomic nitrogen, three distributions are used: N(2) given by Barth (1961) represents the lower limit; N(1) obtained by extrapolating downwards the photochemical distribution recently derived by Ghosh (1968) for heights above 100 km; N(3) representing the upper limit and given by Khovistok (1962) (Fig. 5). The temperature-dependent NO production process $(N+O_2)$ and production through $O_2(^1\Delta)$ compete in importance at heights below 80 km, for k values between 10^{-13}-10^{-15} cm^3/s; the uncertainty in the value of k makes it difficult to judge which is more important. The

former may exceed latter at times of greatly increased temperature and for low k-values. Above 80 km, production through process (N+0) begins to contribute, with a seasonal variation following that of n(0). The ionic process ($O_2^+ + N_2$) is unlikely to be important at any height excepting for very low concentrations of atomic nitrogen. If n(N) is $10^8 cm^{-3}$ or larger at these heights, as seems more likely, this process is never important. Amongst the loss processes (Fig. 4), the most important is (N+NO) for all heights above 70 km (unless atomic nitrogen concentration is as low as in Barth's model), but below 70 km the process ($NO+O_3$) becomes very effective.

There is then a sharp cutoff in NO concentration, the cut-off level, which depends upon the ratio $n(N)/n(O_3)$, is around 60 km for high atomic nitrogen concentration (model 3) but would be as high as 70 km for models 1 and 3.

Since ionospheric estimates yield values around 10^6-$10^7 cm^{-3}$ at 70 km and (less reliably) $5 \times 10^8 cm^{-3}$ at 65 km, the lower cut-off is not acceptable, and the true distribution must at least be equal to, and possibly larger than, that of model 1. The distribution derived from the complete photochemical equation (with the atomic nitrogen distribution of Khovistok and with $k=10^{-14} cm^3/s$) is shown in Fig. 2 along with the ionospheric estimates made in this and the previous works. The agreement

is generally remarkably good except in the region of the minimum where the ionospheric estimates are in agreement with the photochemical values only when process 5 is included. It has also recently been pointed out by Hesstvedt (1968) that when one considers the effect of eddy diffusion there is a tendency for the minimum to be filled up. Our new estimates confirm this. The net result is a nearly constant NO concentration (in the neighborhood of $10^6 cm^{-3}$) all the way from 70 to 100 km.

3. SEASONAL VARIATION IN NITRIC OXIDE

The very high temperature-dependence of NO production through $(N+O_2)$ means that any variations in temperature must profoundly affect the nitric oxide concentration at levels where this process is predominant or competitive, and possibly also at other levels through dynamical forces. It is known that there is a reversal in the seasonal temperature variation (i.e. higher temperature in winter than in summer) from 70 to 90 km, at precisely those heights at which this process can become dominant with increased temperature. CIRA (1965) gives detailed tables of the seasonal variations in temperature at intervals of 10^o in latitude. There will thus be large increases in winter time nitric oxide concentration at medium and high latitudes. In a static atmosphere, this, in turn, would produce large localized regions of enhanced electron density at levels where the $(N+O_2)$ process contributes.

The summer-to-winter changes in nitric oxide as a result of the increase in mesospheric temperature are given in Fig. 6 for two representative latitudes 50^{o}N and 60^{o}N, and represent conditions on January 1 and July 1. NO production through metastable $0_2(^1\Delta)$ is included and its coefficient is assumed to have a value of $10^{-14}cm^3/s$, independent of temperature. If the loss of NO through process $(NO+0_3)$ is ignored, one finds a decrease in nitric oxide concentration from summer to winter from $6x10^8cm^{-3}$ to $5x10^7cm^{-3}$ at 60 km at 60^{o}N latitude and from $3.5x10^8cm^{-3}$ to $5.5x10^7cm^{-3}$ at 50^{o}N, the decrease being roughly a factor of 10 at all heights below 60 km. Above about 67 km, however, the situation is drastically different. At these heights there is a rapid increase in NO concentration; the increase is almost 1 order of magnitude at 75 km, and similar at 80 km. This large increase in NO concentration at altitudes above 67 km continues up to about 90 km. The entire seasonal variation in NO concentration for 50^{o}N is shown in Fig. 7. The large enhancement in NO concentration from October to March has a striking resemblance to HF absorption for similar latitude areas.

4. IONOSPHERIC IMPLICATIONS OF WINTER ENHANCEMENT IN NITRIC OXIDE

These large enhancements in NO concentration at medium and high latitudes has serious implications in D region ionization and especially in its seasonal variation. At 75 km and at 50^{o}N, q(NO) jumps from a value of $4x10^{-2}cm^{-3}sec^{-1}$ in July to

about $30 \times 10^{-2} cm^{-3} sec^{-1}$ in January if production through $O_2(^1\Delta)$ is ignored, and from $30 \times 10^{-2} cm^{-3} sec^{-1}$ in July to about $38 \times 10^{-2} cm^{-3} sec^{-1}$ in January if $O_2(^1\Delta)$ process (with a rate coefficient of $10^{-14} cm^3 sec^{-1}$) is included. As will be seen in Fig. 7, q(NO) is large over the entire period October to March. At $60^{\circ}N$, with $O_2(^1\Delta)$ process, q(NO) has a nearly constant value of $20 \times 10^{-2} cm^{-3} sec^{-1}$ from February to November, with some increase at the equinoxes and somewhat lower values in January and December.

In the summer mesosphere and when NO production through $O_2(^1\Delta)$ is negligible, the X ray contribution exceeds the contribution due to $L\alpha$ at 80 km, during all phases of solar activity, if NO concentration is not much in excess of that given by curve 1 in Fig. 2. With a predominating X-ray source, the winter production rate would then be reduced by a factor of about 5×10^{-2} at $50^{\circ}N$. However, the large enhancement in nitric oxide concentration in winter, yielding a production rate of $8 \times 10^{-1} cm^{-3} sec^{-1}$ in January entirely reverses the situation. The total rate of electron production at 80 km, as a result of this, becomes $8 \times 10^{-1} cm^{-3} sec^{-1}$ in winter against $6 \times 10^{-2} cm^{-3} sec^{-1}$ in summer. One would thus expect a four fold increase in electron density in winter from the enhancement of nitric oxide alone. When $O_2(^1\Delta)$ process is included (with $k = 10^{-14} cm^3/s$ and assumed independent of temperature), $L\alpha$ is found to dominate both summer and winter ionization at 80 km, but winter production rate continues to be high, although now only twice as high as in summer. At lower altitudes, the wintertime enhancement in nitric oxide

becomes progressively smaller and consequently the winter electron density will approach the summer value and will ultimately fall below it.

TABLE 3

WINTER ANOMALY AT 50^{o}N DUE TO NITRIC OXIDE ENHANCEMENT

	SUMMER (27^{o})	WINTER (73^{o})
$q(L\alpha)$	8×10^{-3} (4.6×10^{-1}**)	8×10^{-1} cm^{-3} sec^{-1} (10×10^{-1}**)
$q(X)$	5×10^{-2}	2×10^{-4} cm^{-3} sec^{-1}
q(total)	6×10^{-2} (5×10^{-1}**)	8×10^{-1} cm^{-3} sec^{-1} (10×10^{-1}**)
N_e*	3.5×10^{2} (1×10^{3}**)	3×10^{3} cm^{-3} (1.4×10^{3}**)

*$\psi=5\times10^{-7}$ cm^{3}/s **Including $O_2(^1\Delta)$ process

Two recent experimental observations, relevant to the above discussion, are (i) the electron density profiles of Gregory (1968) obtained with partial reflection at 44^{o}S location and (ii) the observations made by Ferraro and Lee (1967) at the Pennsylvania State University (40^{o}N) during the IQSY with the cross modulation experiment. The Penn State results, although showing considerable scatter, show no evidence of winter anomaly, and is consistent with the variation expected from ionization by X-rays alone. Gregory's observations showing winter electron densities as large as in summer would be consistent with a wintertime enhancement of the type mentioned above, but by a smaller magnitude.

It is also important to note that the winter enhancement in nitric oxide is limited to heights above 70 km, below which the winter mesosphere is cooler than the summer mesosphere. The sharp decrease in NO concentration due to the rapid loss of NO through O_3 can raise this level to about 75 km in case of low atomic nitrogen concentration. Present evidence indicating that the winter anomaly is essentially confined to height between 80-90 km (Gregory, 1968; Sechrist et al, 1968) is in agreement with this.

REFERENCES

Barrington, R. R., Thrane E. V. and Bjelland, B., Canad. J. Phys. 41, 271, 1963.

Barth, C. A., Nitrogen and Oxygen Reactions in the Atmosphere, in: Chemical Reactions in the Lower and Upper Atmosphere (Interscience Publisher), 303, 1961.

Barth, C. A., Ann. Geophys., 22, 198, 1966.

Bowling, T. S., Norman, K., Willmore, A. P., Planet. Space Sci., 15, 1035, 1967.

Deeks, D. G., Proc. Roy. Soc. A., 291, 413, 1966.

Evans, W. F. J., Hunten, D. M., Llewellyn, E. J., and Vallance Jones, A., J. Geophys. Res. 73, 2885, 1968.

Ferraro, A. J., and Lee, H. S., Scientific Reports 308(D) and 312(D), Ionosphere Research Laboratory, Pennsylvania State University, 1967.

Ghosh, S. N., J. Geophys. Res., 73, 309, 1968.

Hunten, Donald M., and McElroy, Michael B., J. Geophys. Res., 73, 2421, 1968.

Maeda, K. I., and Aikin, A. C., Goddard Space Flt. Ctr. Rept. X-640-67-29, Jan. 1967.

Mitra, A. P., J. Atmosph. Terr. Phys., 28, 945, 1966.

Mitra, A. P., J. Atmosph. Terr. Phys., 1968, in press.

Narcisi, R. S. and Bailey, A. D., J. Geophys. Res., 10, 3687, 1965.

Nicolet, M., J. Geophys. Res. 70, 679, 1965; Ibid, 691.

Smith, L. G., J. Atmosph. Terr. Phys., 28, 1195, 1966.

Thrane, E. V., Hang A., Bjelland, B., Anastassiades M., and Tsagakis, E., J. Atmosph. Terr. Phys., 30, 135, 1968.

Wagner Ch-V., J. Atmosph. Terr. Phys., 28, 607, 1966.

LEGEND OF FIGURES

Fig. 1 - Plots of N^2 (proportional to the electron production rate) against log sec χ at selected heights of 65, 70 and 75 km. Electron density observations are those by Thrane et al (1968). Solid lines and theoretical variations of $q(L\alpha)$ with sec χ, and the dotted line for 75 km is the variation of the electron production rate due to 4A alone.

Fig. 2 - Different ionospheric estimates of mesospheric nitric oxide, along with two photochemical distributions one with and the other without the $O_2(^1\Delta)$ process. The dotted portion of the theoretical curves shows the effect of rapid loss of NO through O_3 for the atomic nitrogen distribution of Khostikov.

Fig. 3 - Relative magnitudes of the specific rate of production of NO through different processes (expressed per nitrogen atom). For the ionic reaction $O_2^+ + N_2 \rightarrow NO^+ + NO$, an upper limit of $10^{-15} cm^3/s$ has been used for the rate coefficient. The two curves refer to the atomic nitrogen models N(1) and N(2) in Fig. 4. The corresponding curve for N(3), will be smaller than that for N(1).

Fig. 4 - Assumed distributions of atomic nitrogen and ozone in the mesosphere.

Fig. 5 - Relative magnitudes of the NO loss rates for different reaction, (expressed per NO molecule). The two curves for (N+NO) refer to the atomic nitrogen distributions N(1) and N(2) in Fig. 4.

Fig. 6 - Calculated NO distributions for January and July in the mesosphere corresponding to CIRA temperatures. The sharp cut-offs at the lower levels, different for different atomic nitrogen distributions, should be noted. Production of NO through $[N+O_2(^1\Delta)]$ is included with constant rate coefficient of $10^{-14}cm^3/s$.

Fig. 7 - Seasonal variation of nitric oxide and the resulting electron production rates calculated for 50^oN and for a level of 75 km. Calculation are given for: (a) $N+O_2(^1\Delta)$ process negligible and (b) a temperature-independent rate of $10^{-14}cm^3/s$ for the process $N+O_2(^1\Delta) \rightarrow NO+O$.

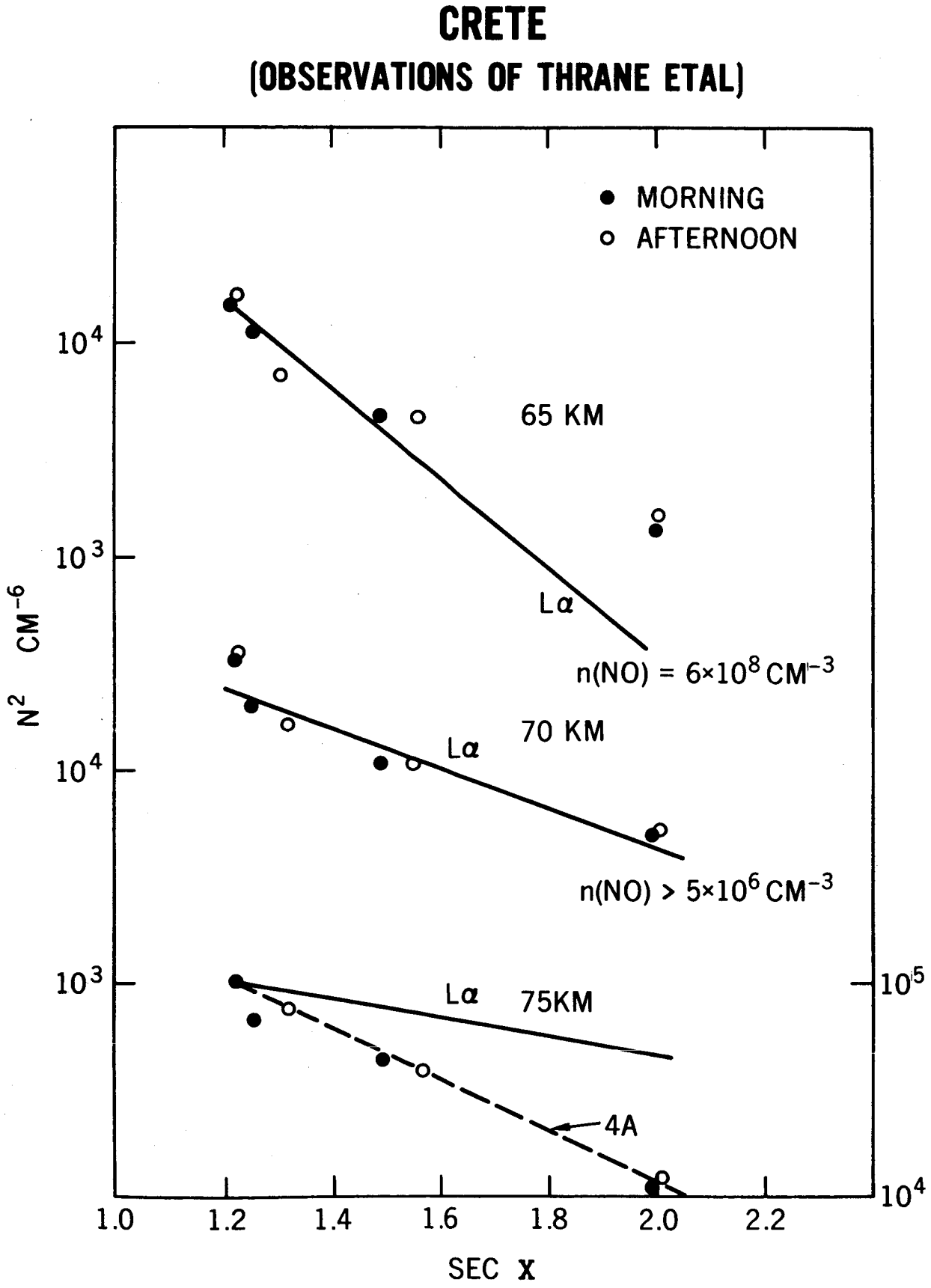
CRETE
(OBSERVATIONS OF THRANE ETAL)
MORNING
AFTERNOON
65 KM
Lα
n(NO) = 6×10^8 CM^-3
70 KM
Lα
n(NO) > 5×10^6 CM^-3
Lα
75KM
4A
N^2 CM^-6
10^4
10^3
10^4
10^3
10^5
10^4
1.0
1.2
1.4
1.6
1.8
2.0
2.2
SEC X

Figure 1

AVERAGE DISTRIBUTION

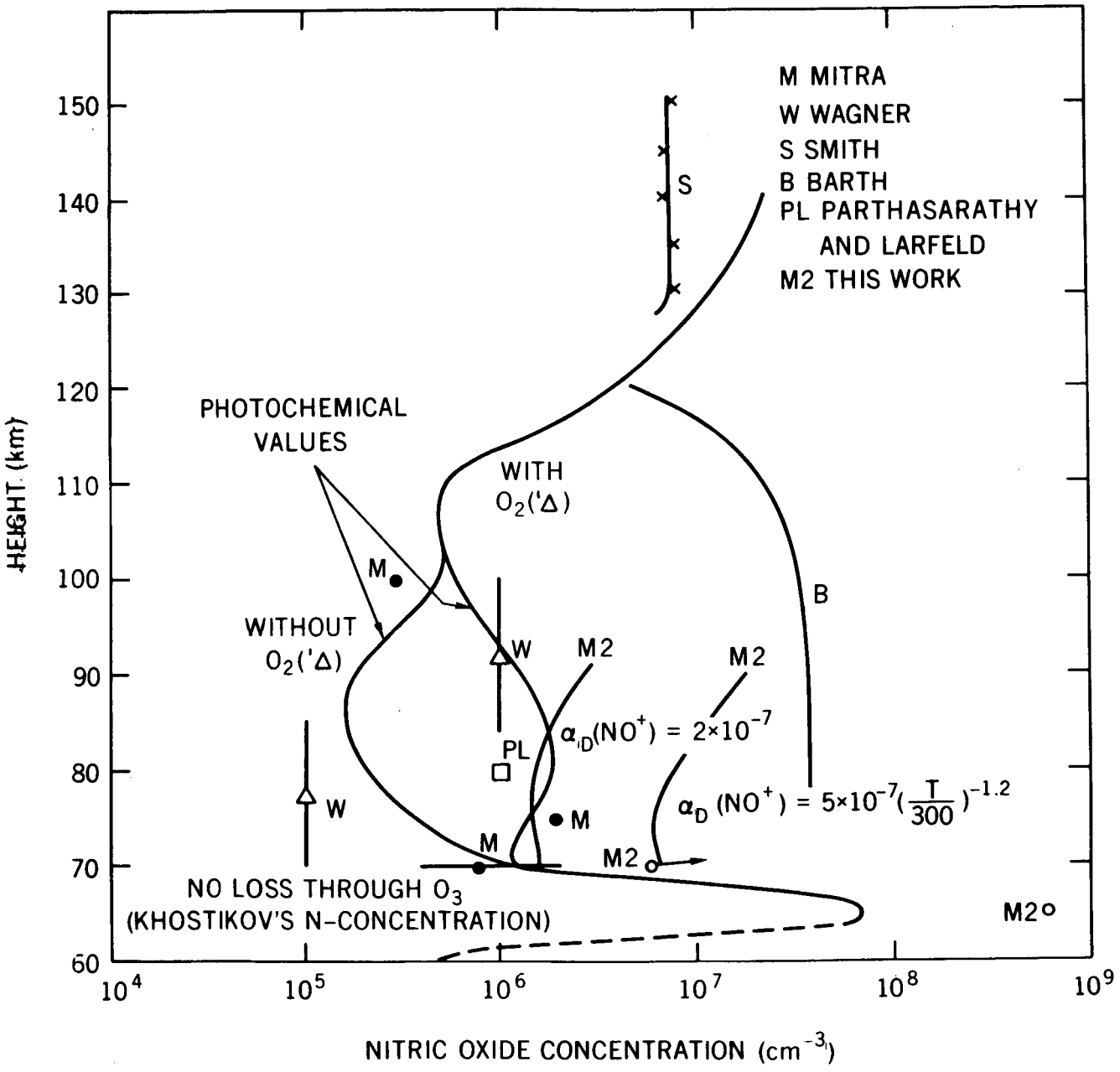

Figure 2

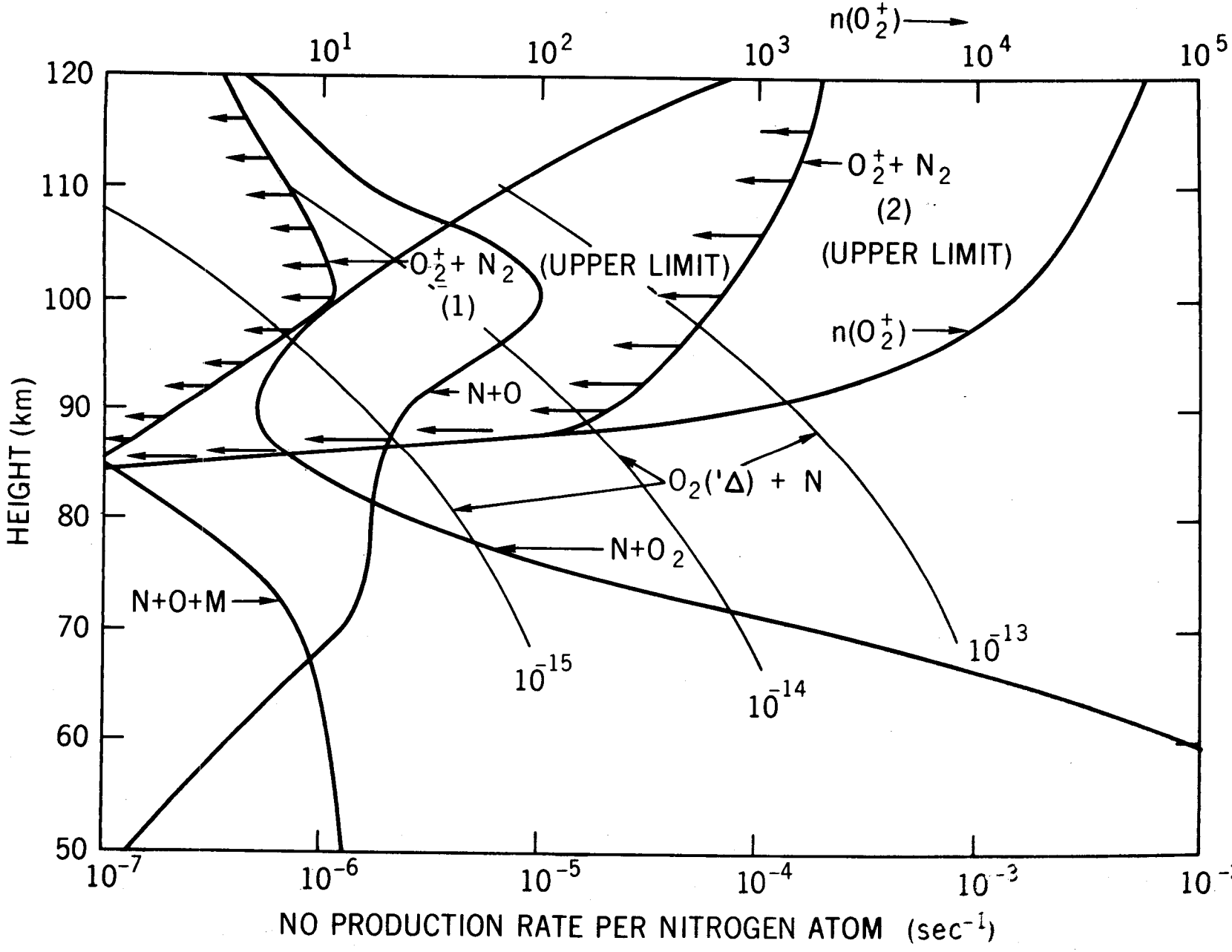
$n(O_2^+)$
10^1
10^2
10^3
10^4
10^5
120
110
100
90
80
70
60
50
HEIGHT (km)
$O_2^+ + N_2$ (1)
(UPPER LIMIT)
$O_2^+ + N_2$ (2)
(UPPER LIMIT)
$n(O_2^+)$
N+O
$O_2('\Delta) + N$
$N+O_2$
N+O+M
10^{-15}
10^{-14}
10^{-13}
10^{-7}
10^{-6}
10^{-5}
10^{-4}
10^{-3}
10^{-2}
NO PRODUCTION RATE PER NITROGEN ATOM (sec^{-1})

Figure 3

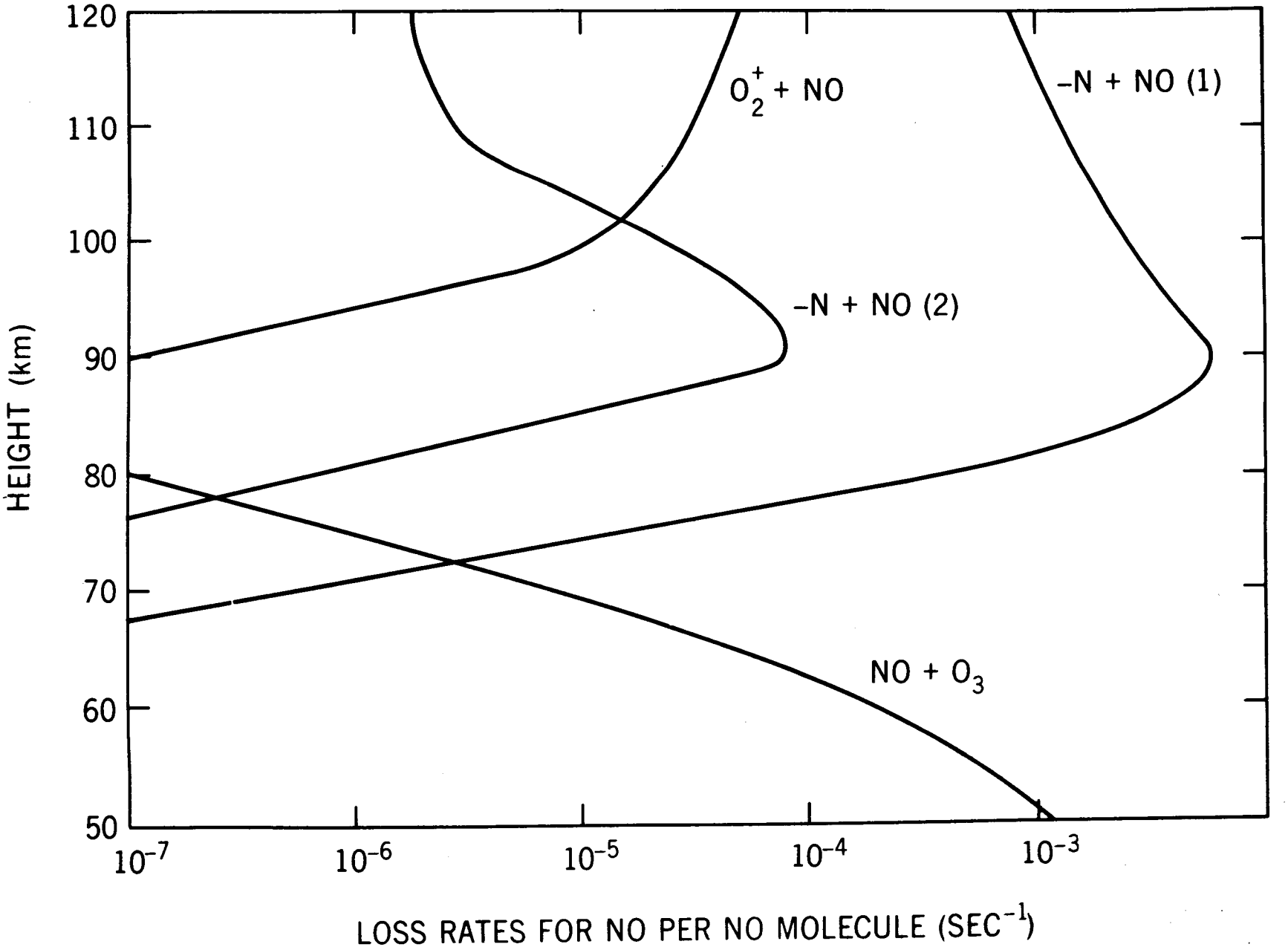
120
110
100
90
80
70
60
50
HEIGHT (km)
$O_2^+ + NO$
–N + NO (1)
–N + NO (2)
NO + O_3
10^{-7}
10^{-6}
10^{-5}
10^{-4}
10^{-3}
LOSS RATES FOR NO PER NO MOLECULE (SEC^{-1})

Figure 4

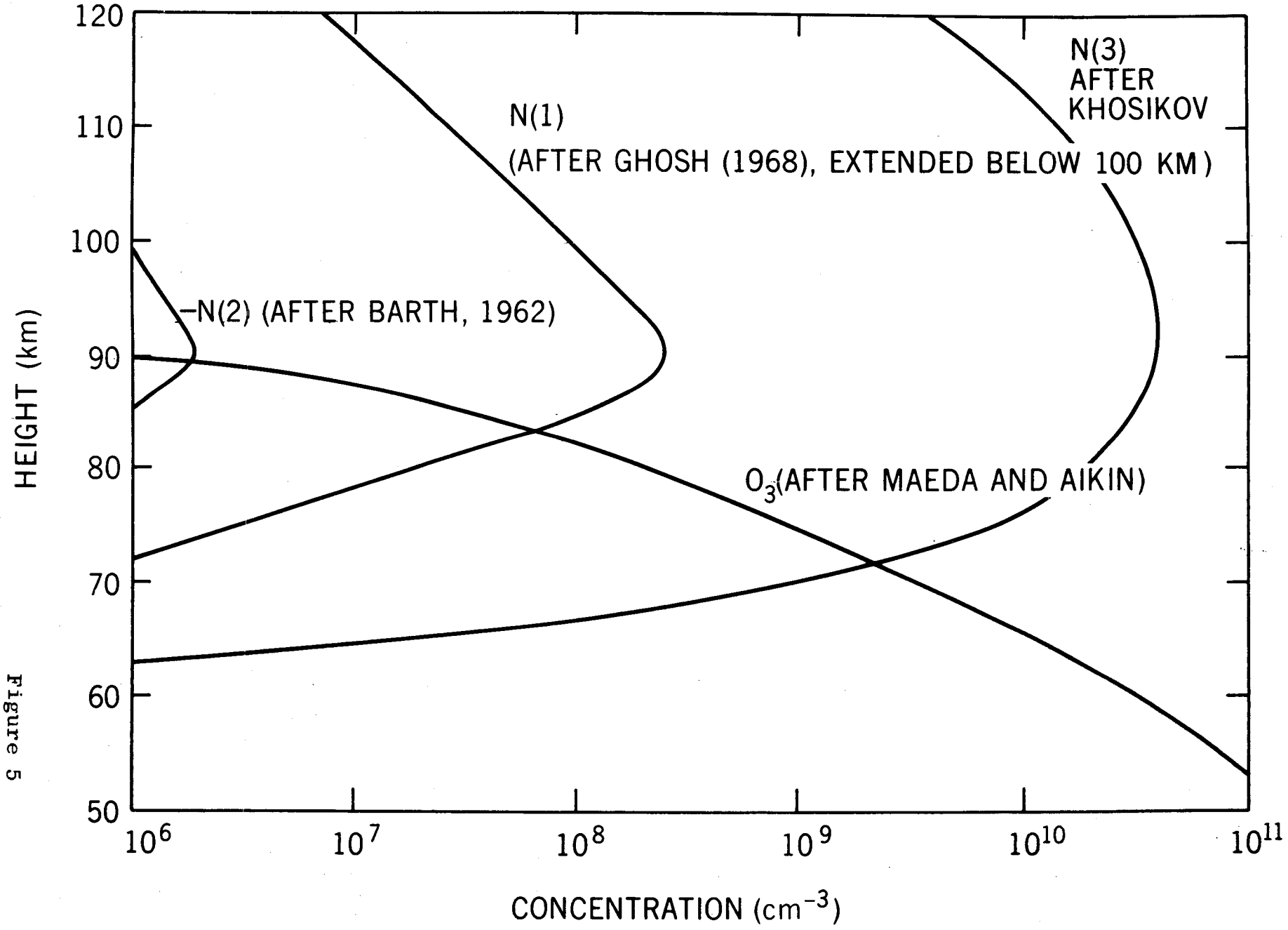
120
110
100
90
80
70
60
50
HEIGHT (km)
N(1)
(AFTER GHOSH (1968), EXTENDED BELOW 100 KM)
N(3)
AFTER
KHOSIKOV
N(2) (AFTER BARTH, 1962)
O_3(AFTER MAEDA AND AIKIN)
10^6
10^7
10^8
10^9
10^{10}
10^{11}
CONCENTRATION (cm^{-3})

Figure 5

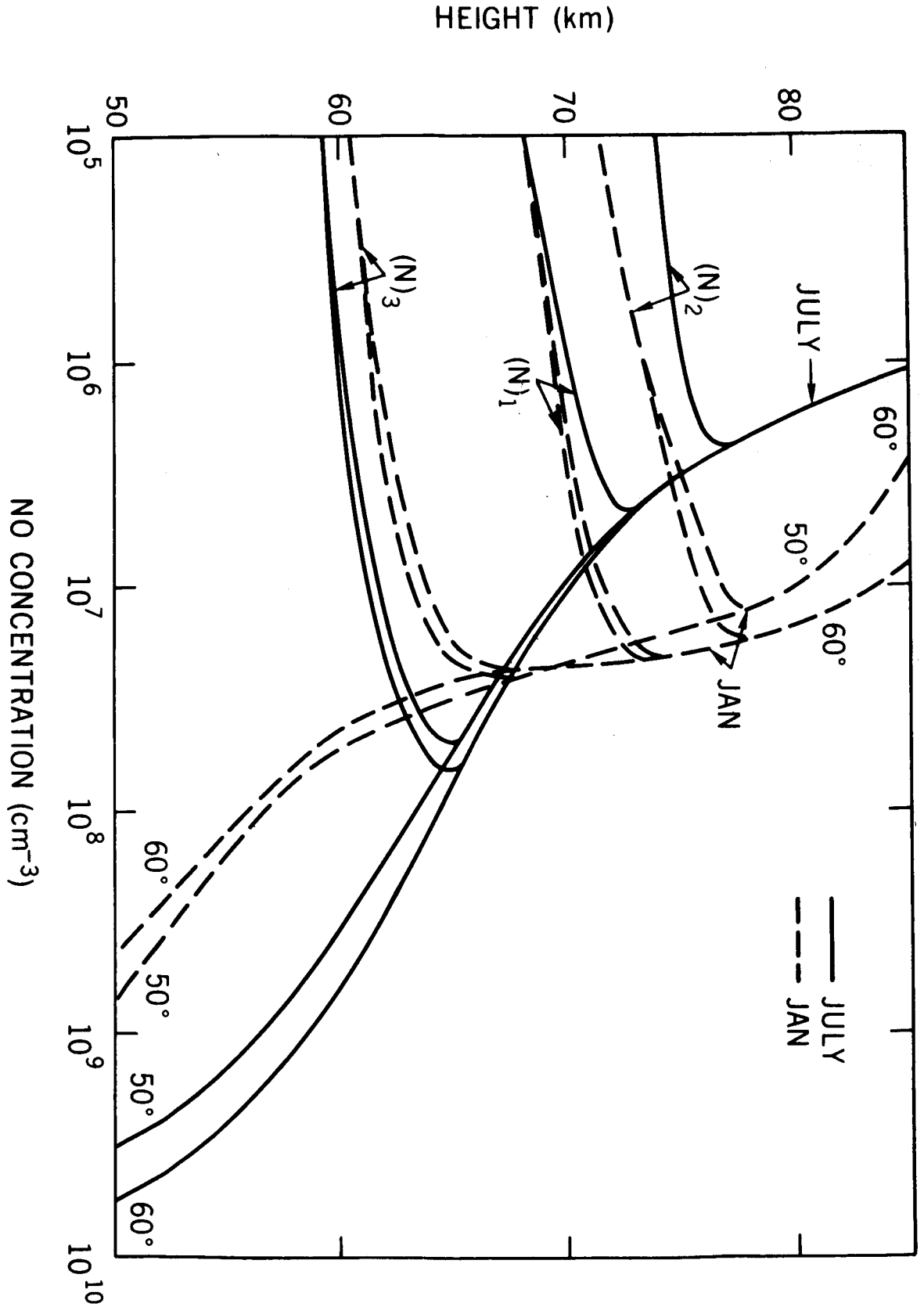
HEIGHT (km)
50
60
70
80
10^5
10^6
10^7
10^8
10^9
10^{10}
NO CONCENTRATION (cm^{-3})
$(N)_3$
$(N)_2$
$(N)_1$
JULY
JAN
60°
50°
60°
60°
50°
50°
60°
JULY
JAN

Figure 6

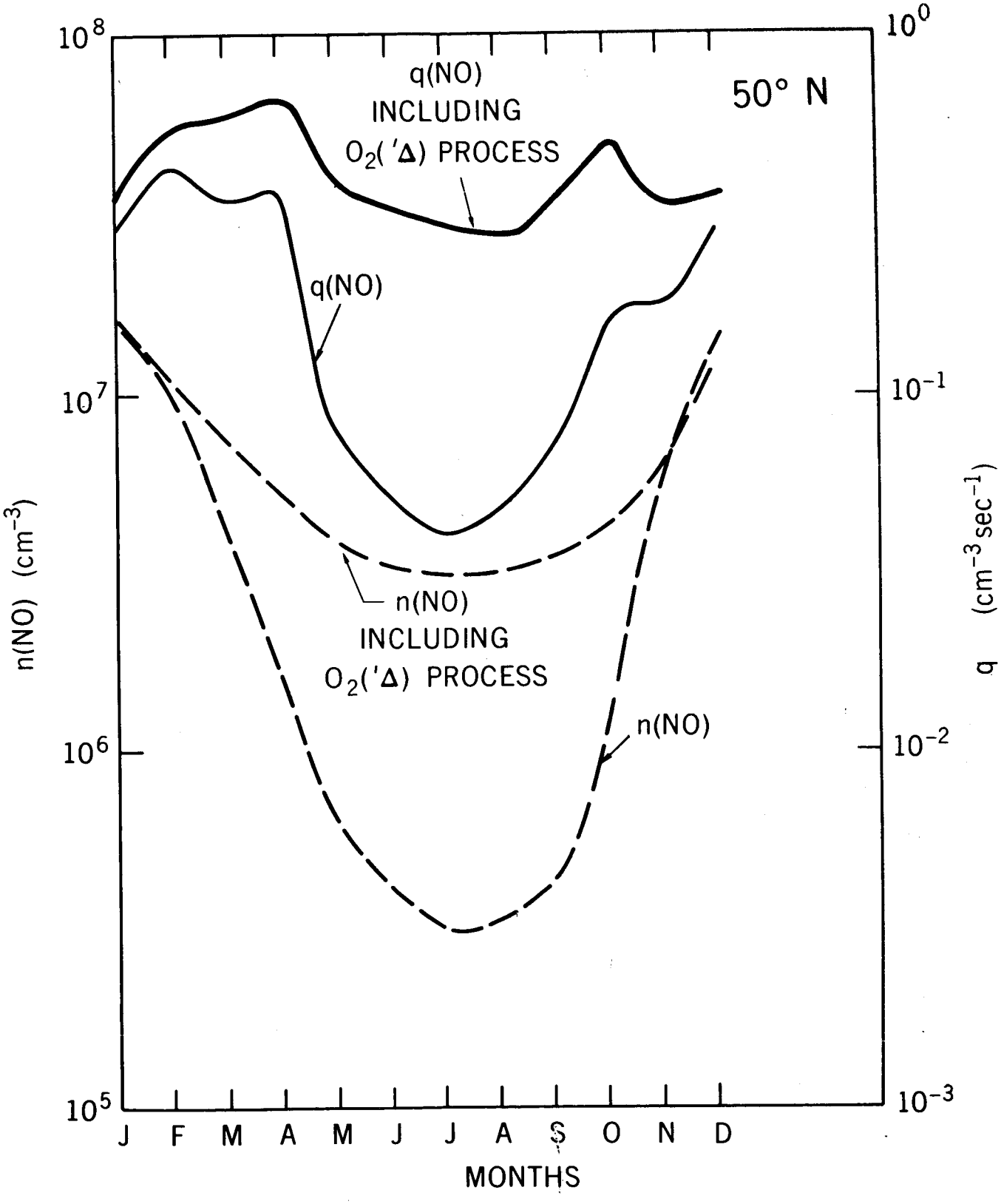
75 KM
50° N
q(NO)
INCLUDING
$O_2(^1\Delta)$ PROCESS
q(NO)
n(NO)
INCLUDING
$O_2(^1\Delta)$ PROCESS
n(NO)
10^8
10^7
10^6
10^5
10^0
10^{-1}
10^{-2}
10^{-3}
n(NO) (cm^{-3})
q ($cm^{-3}sec^{-1}$)
J F M A M J J A S O N D
MONTHS

Figure 7

APPENDIX 1

ESTIMATES OF NITRIC OXIDE CONCENTRATION IN D AND E REGIONS

METHOD	PROCEDURE	NITRIC OXIDE CONCENTRATION cm^{-3}	NITRIC OXIDE HEIGHT km	AUTHORS
IONOSPHERIC METHODS	1. FROM SOLAR CYCLE VARIATION IN N_e	8×10^5 (RANGE 4×10^5 -2×10^6)	70	MITRA (1966)
	2. FROM DIURNAL VARIATION IN N_e	$\frac{n(NO)}{n(O_2)} \approx 10^{-8}$ Giving 2×10^6 at 75km	70–75	MITRA (1968)
	3. FROM NO^+, O_2^+ MEASUREMENTS	a. 2×10^6	75	} MITRA (1968)
		(3×10^5)	100 (1)	
		b. $< 10^5$	70–84	} WAGNER (1966)
		10^6	84–100	
	4. ZENITH ANGLE VARIATION IN ABSORPTION	1×10^6 (1)	80	PARTHASARATHY AND LARFELD (1965)
	5. SIMULTANEOUS MEASUREMENTS OF N_e AND L_α FLUX NEAR TWILIGHT	$(8 \pm 1) \times 10^6$	130–150	SMITH (1966)
ROCKET	NO AIRGLOW	6×10^7	75–95	BARTH (1966)
		1.5×10^7	120	
PHOTO–CHEMICAL VALUES	FROM LABORATORY MEASUREMENTS OF RATE COEFFICIENTS	1.8×10^6	75	KRISTIAKOWSKY AND VOLPI
		5.5×10^5	120	
		2×10^6	75	MAVORAYANNIS AND WINCKLER
		1×10^6	120	
		3.5×10^6	75	CLYNE AND THRUSH
		1.3×10^6	120	

(1) USING $\alpha_i = 2 \times 10^{-7} cm^3/s$